J Neuroimmune Pharmacol
DOI 10.1007/s11481-012-9346-3

BRIEF REPORT

# Near-field Quantification of Complement Receptor 1 (CR1/CD35) Protein Clustering in Human Erythrocytes

**Zachary J. Lapin · Christiane Höppener · Harris A. Gelbard · Lukas Novotny**

Received: 31 August 2011 / Accepted: 9 February 2012


**Abstract** We investigate the distribution of the membrane protein complement receptor 1 (CR1/CD35) in human erythrocyte membrane ghosts using scanning near-field optical microscopy. Recent studies have demonstrated that levels of Aβ peptide, associated with Alzheimers disease (AD) and present in brain and peripheral blood, vary significantly when bound by complement C3b-dependent adherence to CR1. It is unknown why patients with AD have a markedly impaired ability to bind Aβ to CR1 via this mechanism, but one possibility is a defect in the localization and/or conformation of CR1 in the membrane. Scanning near-field optical microscopy does not require the harsh preparation of electron microscopy techniques and may therefore be better suited for measuring membrane protein distributions. The clustering phenomenon of CR1 identified in electron microscopy studies is confirmed and quantified. The standard deviation of the inter-cluster spacing of CR1 is constant ($79 \pm 9$ nm) across erythrocytes with between 61 and 124 clusters per membrane ghost.

**Keywords** Alzheimer's disease · Complement receptor 1 (CR1/CD35) · Membrane protein · Nearfield microscopy · SNOM · Protein distribution mapping

## Introduction

Alzheimer's disease (AD) is a terminal neurodegenerative disease that generally afflicts older individuals. The exact cause of late-onset AD is still unknown, although there are characteristic abnormalities in the brains of patients with AD. Attempts to treat the symptoms of AD directly has had little effect on the progression of the disease, however, treating the underlying cause of these abnormalities may be more fruitful. Genetic risk factors for familial AD are already known (Waring and Rosenberg 2008) and recent studies have found risk factors for late-onset AD as well.

Complement receptor 1 (CR1/CD35) is a type 1 transmembrane glycoprotein that several studies have implicated as a possible risk factor for developing AD (Crehan et al. 2011). CR1 is predominantly expressed in erythrocytes, with as many as 1,300 CR1 per cell (Walport et al. 1985). The role of CR1 is to clear immune opsonized complexes and deliver them to the liver for degradation (Hess and Schifferli 2003). One specific example of this is that free amyloid-beta ($A\beta_{1-42}$) peptides are quickly bound by C3b, followed by CR1, to be removed from the brain

This work has been supported by the National Science Foundation (CBET-0930074) and a University of Rochester Provost's Multi-Disciplinary Award.

Z. J. Lapin · L. Novotny (✉)
Institute of Optics, University of Rochester,
Rochester, NY 14627, USA
www.nano-optics.org

C. Höppener
Institute of Physics, University of Muenster,
48149 Muenster, Germany

H. A. Gelbard
Center for Neural Development & Disease and
Department of Neurology (Child Neurology Division),
University of Rochester Medical Center,
Rochester, NY 14627, USA

Published online: 29 February 2012

(Rogers et al. 1992). The accumulation of $A\beta_{1-42}$ in the brain, a pathologic hallmark of AD, is not alone sufficient to cause AD.

One major finding to implicate abnormalities in CR1 in patients with AD is a negative correlation between level of cognitive impairment and the amount of bound $A\beta_{1-42}$ within erythrocytes (Rogers et al. 2006). Genetic studies support that CR1 may play a role in the development of AD. A genome-wide association study found variants of CR1 that were associated with AD (Lambert et al. 2009). Four single nucleotide polymorphisms (SNPs) near CR1 have also been correlated with increased levels of $A\beta_{1-42}$ in cerebrospinal fluid (CSF), suggesting that these SNPs affect the ability for CR1 to effectively bind $A\beta_{1-42}$ (Brouwers et al. 2012). The exact impact of the SNPs is unknown and therefore it is necessary to understand the relationship between CR1 function and expression within human erythrocytes.

Protein distributions are often imaged with electron microscopy (EM), a powerful technique that uses electrons to map nanometer-scale features. Two EM studies of CR1 have been performed and both have revealed a clustering nature of CR1 within human erythrocyte membranes (Chevalier and Kazatchkine 1989; Paccaud et al. 1988). Unfortunately, EM studies are not ideal; the necessary toxic fixative agents (e.g. gludaraldehyde, paraformaldehyde, $OsO_4$, etc.) and the harsh imaging environment (e.g. vacuum, high energy electrons, etc.) may alter the native distribution of proteins under investigation. Additionally, the physical size of the required immunogold labels may further disrupt the native or pathophysiologic conformation of the protein. In general, it is assumed that EM studies do preserve the key aspects of a biological system being studied, but disparities between fixed and unfixed samples still cause concern with this technique.

Imaging with optical light is ideal due to the inherent compatibility between biological organisms and light; however, standard optical imaging techniques have a resolution limited to a few hundred nanometers—the diffraction limit. As we show, the resolution provided by standard optical techniques is insufficient to resolve the cluster distribution of CR1 within the erythrocyte membrane. Scanning near-field optical microscopy (SNOM) is a powerful technique that allows for sub-diffraction optical resolution while simultaneously providing a topographical image that can be correlated with the optical measurement (Novotny and Hecht 2006). SNOM, in its various forms, has been applied to a range of biological questions. The methods used within this paper have previously been demonstrated for biological applications by the near-field mapping of the plasma membrane $Ca^{2+}$ 1(PMCA1) distribution in human erythrocytes (Hoeppener et al. 2009).

## Methods

Biological samples were prepared similarly as described by Hoeppener and Novotny (Hoeppener and Novotny 2008). Blood was provided by a healthy male in his mid-twenties with no signs of or family history of dementia. Erythrocytes were isolated from ~50 μL of human blood by centrifugation in an ice cold 150 mM KH buffer (150 mM potassium chloride, 20 mM HEPES, 24 mM sucrose; pH 7.4). The erythrocytes were diluted 30-fold with the KH buffer and 300 μL of erythrocytes were placed on an APTES (3-aminopropyltriethoxy-silane) functionalized coverslip, allowing a monolayer of cells to adhere to the coverslip. After rinsing, ~200 μL of 2% w/w solution of BSA (bovine serum albumin cohn-V fraction) in the KH buffer was placed on the coverslip for 3 h to reduce future nonspecific labeling of the remaining exposed APTES functionalized substrate.

The cells were then lysed with a 0.2% w/w solution of BSA in a 5 mM sodium phosphate buffer (5 mM $NaH_2PO_4$, 1 mM Free EDTA; pH 7.4) under pressure from a syringe. Membrane ghosts are used to allow the optical antenna to image a rigid surface as well to minimize the background fluorescence of the sample. The exposed cytoplasmic side of the erythrocytes was labeled for CR1 with a H-300 rabbit anti-CR1 primary antibody (Santa Cruz Biotechnology, Santa Cruz, CA), diluted 1:400. Finally, membrane ghosts were labeled with an Alexa Fluor 633 conjugated $F(ab')_2$ goat anti-rabbit antibody (Invitrogen, Carlsbad, CA), diluted 1:800. Both antibodies were placed in the 0.2% w/w solution of BSA in 5 mM sodium phosphate buffer and the samples were washed thoroughly between each step with the appropriate buffer. All samples were kept wet and at room temperature for the entire preparation. Additionally, control samples were prepared by not adding the primary antibody.

Measurements were performed similarly as described previously by Hoeppener et al. (2009). All measurements are made with an investigator-built scanning near-field optical microscope. A Nikon Eclipse TE300 inverted confocal microscope (Nikon, Japan) is modified by placing a investigator-built atomic force microscope (AFM) on top and positioning the AFM probe into the center of the confocal optical focus. The AFM probe is an 80 nm gold sphere (optical antenna) attached to a sharp glass pipet. A 100× NA 1.4 oil-immersion objective (Nikon, Japan) and radially

polarized optical excitation ($\lambda$ = 632.8 nm, power = 50 nW) allows for a strong longitudinally polarized excitation at the center of the optical focus, providing maximum field enhancement from the optical antenna (Anger et al. 2006).

The sample is raster-scanned between the objective and near-field probe. Emitted fluorescence photons are detected by a single photon-counting APD (PerkinElmer, Waltham, MA) for each pixel. The near-field probe is modulated at 100 Hz between ~5 nm and ~65 nm from the sample surface. This modulates the fluorescence rate: increasing the rate when the antenna is close to the surface and decreasing it when the probe is farther away. The measured photon counts are demodulated in a model SR830 lock-in amplifier (Stanford Research Systems, Sunnyvale, CA) at the first harmonic. This technique provides an image of the near-field interaction between the optical antenna and sample (Hoeppener et al. 2009).

Data analysis was performed by isolating fluorescence peaks associated with labeled CR1 in the near-field background suppressed image. To do this, all pixels with a value less than two standard deviations above the mean of the control sample were neglected. The remaining fluorescence peaks were attributed to CR1 clustering and were catalogued by their intensity, physical location, and spatial extent. This information was then used to calculate the Euclidean nearest-neighbor cluster spacing for each cluster.

## Results

Erythrocyte membrane ghosts were created and labeled against CR1. Membrane ghosts have an area of ~45 $\mu m^2$ as determined by the topographic image provided by SNOM, accounting for between one-third and one-half of the surface area of an intact erythrocyte. An optical spatial resolution of 56 nm is achieved allowing the spatial extent of clusters to be measured. Since the antibodies used are only a few nanometers in area, fluorescent peaks with a spatial extent larger than the resolvable optical resolution are due to several closely spaced CR1 proteins, or clusters.

Figure 1 shows corresponding confocal and near-field images along with the spatial extent of each CR1 cluster for a membrane ghost labeled against CR1. The resolution enhancement provided by SNOM is shown to be necessary to resolve CR1 clusters for a given membrane ghost. Peaks with a spatial extent of less than three pixels (~70 nm) could not be attributed to CR1 clustering from control measurements and are not used in subsequent calculations of the inter-cluster spacing distribution of CR1.

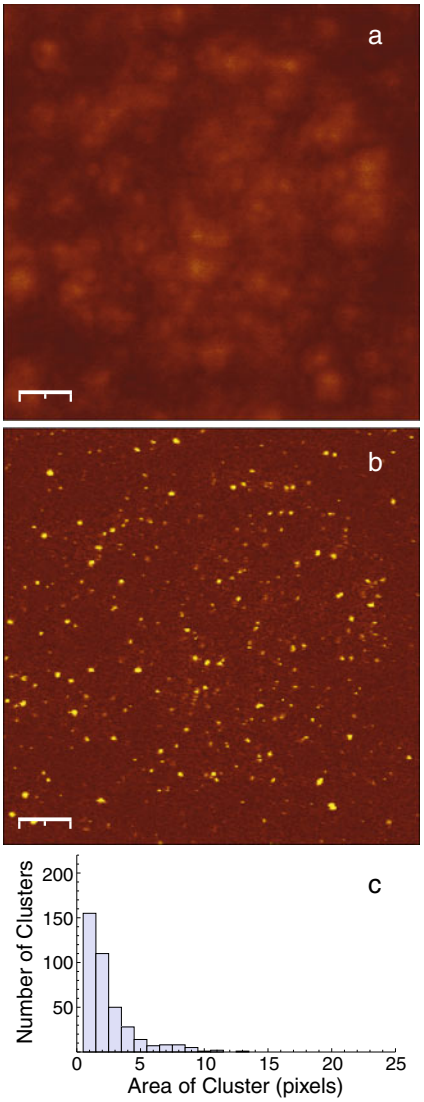


**Fig. 1** Confocal **a** and corresponding background suppressed near-field image **b** for a representative membrane ghosts labeled for CR1 and the corresponding histogram of the area of each fluorescent peak on each membrane ghost **c**. Scale bars are 1 μm. The pixel size is 35 × 35 nm

The inter-cluster spacing of CR1 in four cells is shown in Fig. 2. The number of CR1 clusters per erythrocyte ghost ranged between 61 and 124, with a mean number of 92. Additionally, the mean inter-cluster spacing across all of the cells measured is confirmed to be unresolvable by conventional diffraction limited optical techniques (resolution = $\lambda/2$ >250 nm). The average inter-cluster spacing of CR1 increases with a decrease in number of clusters, which range between 184 and 256 nm. Notably, regardless of the number of measured clusters and the mean inter-cluster spacing

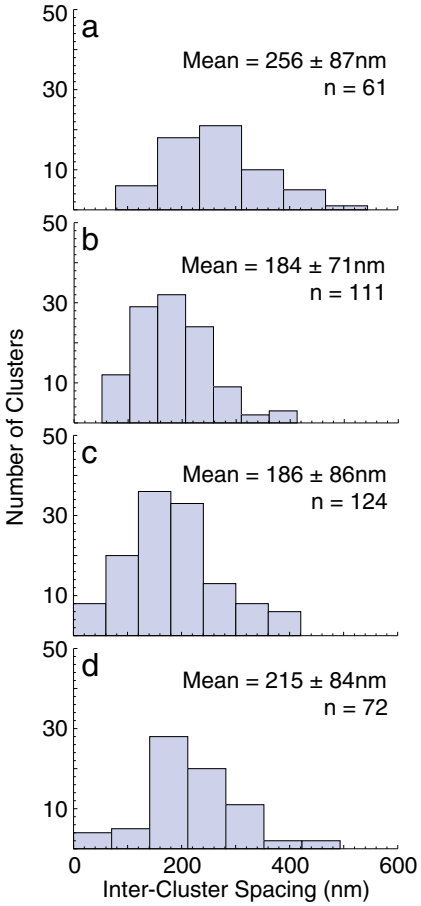


**Fig. 2** The inter-cluster spacing of CR1 in four membrane ghosts. Also given is the mean value and standard deviation of each distribution along with the number of measured clusters with an area greater than three pixels. The pixel size is 35 × 35 nm

(203 ± 85 nm across all membranes), the standard deviation of the inter-cluster spacing remains nearly constant across all four membrane ghosts analyzed, with a value 79 ± 9 nm.

## Discussion

We apply SNOM to quantitatively measure the spatial extent and inter-cluster spacing of CR1 clusters in erythrocytes from a healthy man in his mid-twenties with no symptoms of or family history of dementia. The methods used are designed to optimally preserve the physiological distribution of CR1 within the erythrocyte membrane. Erythrocytes were promptly adhered to an APTES functionalized coverslip, allowing the dense monolayer of APTES to hold lipids and proteins on the surface without chemical fixatives. Additionally, labels are small and all labeling is performed after the membranes are adhered to the surface, preventing any alterations of the physiological CR1 distribution.

The results of this method of biological sample preparation can be compared with that of EM studies. While the clustering nature of CR1 is observed as it was in EM studies, the distributions presented here are different than results previously reported (Paccaud et al. 1988; Chevalier and Kazatchkine 1989). Paccaud et al. (1988) measures an average of 6.7–81.8 CR1 clusters per erythrocyte, with more clusters representative of cells with more CR1 and an average cluster size of ∼4 CR1 per cluster. Chevalier and Kazatchkine (1989) report 3–8 CR1 clusters per erythrocyte with an average of 37 or 67 (for each donor) CR1 per cluster. SNOM is capable of determining the number of proteins per cluster; however, this requires photobleaching experiments or statistical approaches, including photon antibunching, along with the appropriate monoclonal antibodies. We measure the area and number of CR1 clusters in membrane ghosts, and can estimate the total number of CR1 clusters per erythrocyte could be as large as ∼350.

We also quantify the distribution of CR1 within the erythrocyte membrane, revealing the cellular organization of the protein. This is observed by the nearly constant standard deviation of the inter-cluster spacing of CR1. If the clusters were randomly distributed, reducing the number of clusters by a factor of two would increase the standard deviation of inter-cluster spacing by a factor of square root two, which is not observed. The cell is tightly regulating the distribution of CR1 clusters within the membrane.

Although measurements are preformed with dehydrated samples, our sample preparation embraces physiological conditions as much as possible to insure that the measured distributions are the same as the physiological distribution. The differences between SNOM and EM studies as well as inconstancies between fixed and unfixed samples within the EM studies suggests that the method of sample preparation may influence measured distributions. The physiological sample preparation allowed by SNOM measurements may have a significant advantage over EM in probing the physical expression of proteins, such as CR1, that may be affected in disease states.

A continuation of this study to better understand the distribution of CR1 clusters in both healthy individuals and individuals with AD would allow quantitative analyses of any alterations in the expression of CR1 and its correlation with AD to be performed. This could fuel the development of new and accessible biomarkers for patients with mild cognitive impairment and AD.

**Acknowledgements** We are indebted to Professors Paul Coleman and Joseph Rodgers of Sun Health Systems, Tucson, AZ for their insights into the biology of CR1 in patients with AD.

## References

Anger P, Bharadwaj P, Novotny L (2006) Enhancement and quenching of single molecule fluorescence. Phys Rev Lett 96:113002

Brouwers N et al (2012) Alzheimer risk associated with a copy number variation in the complement receptor 1 increasing C3b/C4b binding sites. Mol Psychiatry 17:223–233

Chevalier J, Kazatchkine MD (1989) Distribution in clusters of complement receptor type one (CR1) on human erythrocytes. J Immunol 142:2031–2036

Crehan H, Holton P, Wray S, Pocock J, Guerreiro R, Hardy J (2011) Complement receptor 1 (CR1) and Alzheimer's disease. Immunobiology. doi:10.1016/j.imbio.2011.07.017

Hess C, Schifferli JA (2003) Immune adherence revisited: novel players in an old game. News Physiol Sci 18:104–108

Hoeppener C, Novotny L (2008) Antenna-based optical imaging of single $Ca^{2+}$ transmembrane proteins in liquids. Nano Lett 8:642–646

Hoeppener C, Beams R, Novonty L (2009) Background suppression in near-field optical imaging. Nano Lett 9:903–908

Lambert JC et al (2009) Genome-wide association study identifies variants at CLU and CR1 associated with Alzheimer's disease. Nat Genet 41:1094–1100

Novotny L, Hecht B (2006) Principles of nano-optics. Cambridge University Press, Cambridge

Paccaud JP, Carpentier JL, Schifferli JA (1988) Direct evidence for the clustered natured of complement receptors type 1 on the erythrocyte membrane. J Immunol 141:3889–3894

Rogers J et al (1992) Complement activation by β-amyloid in Alzheimer disease. Proc Natl Acad Sci 89:10016–10020

Rogers J et al (2006) Peripheral clearance of amyloid β peptide by complement C3-dependent adherence to erythrocytes. Neurobiol Aging 27:1733–1739

Walport MJ, Ross GD, Mackworth-Young C, Watson JV, Hogg N, Lachmann PJ (1985) Family studies of erythrocyte complement receptor type 1 levels: reduced levels in patients with SLE are acquired, not inherited. Clin Exp Immunol 59:547–554

Waring SC, Rosenberg RN (2008) Genome-wide association studies in Alzheimer disease. Arch Neurol 65:329–334